POLITECNICO DI TORINO
Repository ISTITUZIONALE

Wideband magnetic losses and their interpretation in HGO steel sheets

(Article begins on next page)

11 February 2024

Wideband magnetic losses and their interpretation in HGO steel sheets

O. de la Barrière [a],[*], E. Ferrara [b], A. Magni [b], A. Sola [b], C. Ragusa [c], C. Appino [b], F. Fiorillo [b]

[a] *Laboratoire SATIE, CNRS–ENS, Saclay, France*
[b] *Advanced Materials Metrology and Life Sciences, Istituto Nazionale di Ricerca-Metrologica-INRIM, 10135 Torino, Italy*
[c] *Energy Department, Politecnico di Torino, 10129 Torino, Italy*

ABSTRACT

The magnetic properties of high-permeability grain-oriented (HGO) Fe-Si sheets have been investigated in the frequency range 1 Hz-10 kHz, with attention devoted to the role of thickness on the behavior of the magnetic losses and the phenomenology of skin effect. The study is focused on the wideband response of 0.174 mm and 0.289 mm thick sheets, comparatively tested at peak polarization values ranging between 0.25 T and 1.7 T. The experiments associate fluxmetric measurements with direct Kerr observations of the dynamics of the domain walls. A picture of the magnetization process comes to light, where the dynamics of the flux reversal takes hold under increasing frequencies through the motion of increasingly bowed 180° walls, eventually merging at the sheet surface for a fraction of the semi-period. This effect can be consistently predicted, starting from the Kerr-based knowledge of the equilibrium wall spacing, by the numerical modeling of the motion of an extended array of 180° domain walls, subjected to the balanced action of the applied and eddy current fields, and the elastic reaction of the bowed walls. This model can be incorporated into the general concept of loss separation, by calculating the classical loss component through the solution of the Maxwell's diffusion equation under a magnetic constitutive law identified with the normal DC curve. The numerical domain wall model and the loss decomposition consistently predict that the excess loss component, playing a major role in these grain-oriented materials at power frequencies, tends to disappear in the upper induction-frequency corner.

1. Introduction

High-permeability grain oriented (HGO) Fe-Si sheets have slowly and steadily improved their magnetic properties since their introduction in the seventies [1]. Better material purity and reduced density of defects, domain refinement by laser scribing, and decreased sheet thickness without loss of crystallographic perfection have been achieved along the years and products with power loss figure lower than 1.0 W/kg at 50 Hz and 1.7 T peak induction are nowadays available [2–4]. With present-day evolution in transformer applications, such as those connected with the development of smart distribution grids and efficient power conversion in traction [5,6], where medium frequencies and non-sinusoidal voltages are involved, special interest is attached to the use of the recently developed thin ($d = 0.18 – 0.20$ mm) HGO laminations. They appear ideal, for example, for the working frequencies and induction waveforms of solid-state transformers and transformers employed in DC-DC converters [7,8]. However, by moving the frequencies in the kHz range, we are faced with novel requirements regarding the precise characterization of the HGO sheets and of

inductive cores [9,10], whereas solidly assessed concepts routinely applied in the theoretical interpretation of the magnetic losses at power frequencies need to be revisited, in the light of a remarkable evolution of the dynamics of the domain walls (dws) and the progressively reduced penetration of the magnetic flux across the sheet core. The question is therefore posed regarding the way one can consistently fit the decrease of the skin depth in a mechanism for the unfolding of the dw motion under increasing frequency and how this is quantitively reflected in the corresponding evolution of the energy loss $W(f)$. This quantity is theoretically assessed in GO sheets, up to frequencies where the assumption of near-uniform flux through the sheet depth holds, by the Statistical Theory of Losses (STL). It is a physical model, which provides a full interpretation, through the quantitative derivation of the loss components, of the dependence of $W(f)$ on frequency and peak polarization J_p [11,12]. Remarkably, STL equally applies to non-oriented and grain-oriented steel sheets. Some criticism was raised in the recent literature concerning the adopted simple formulation of the classical loss component $W_{class}(f)$ under standard conditions (full flux penetration) and high J_p values [13,14]. It was experimentally shown, however, that

---

* Corresponding authors.
E-mail address: olivier.de-la-barriere@ens-paris-saclay.fr (O. de la Barrière).

the suggested alternative approach, the so-called saturation-wave-model, overestimated the measured loss in non-oriented sheets [15], while it was originally demonstrated that, by treating the motion of the 180° dws in statistical terms, distinct classical and excess $W_{exc}(f)$ contributions can always be identified in HGO sheets [12]. It is apparent, in fact, that, even in the presence of well-defined arrays of 180° dws, one cannot get rid of a statistical distribution of the pertaining variables in actual GO sheets. Renouncing to the separate identification of $W_{class}(f)$ and $W_{exc}(f)$, as proposed in [14], can be seen as a possible alternative. However, the prediction of the dynamic loss $W_{dyn}(f) = W_{class}(f) + W_{exc}(f)$ requires in this case a far from simple retrieval of J-dependent fitting parameters from pre-emptive measurements. Of course, at frequencies sufficiently high to hinder flux penetration, the following standard formulation for the classical loss (assuming induction and polarization to coincide) in a lamination of thickness d and conductivity σ

$$W_{class}(f) = \frac{\pi^2}{6}\sigma J_p^2 d^2 f \quad [\text{J/m3}] \tag{1}$$

does not hold, as well as the closed expression obtained as solution of the Maxwell's diffusion equation in a hypothetical linear medium of defined permeability μ

$$W_{class}(f) = \frac{\pi}{2}\frac{\gamma J_p^2}{\mu}\frac{\sinh\gamma - \sin\gamma}{\cosh\gamma - \cos\gamma}, \quad [\text{J/m}^3] \tag{2}$$

where $\gamma = \sqrt{\pi\sigma\mu d^2 f}$. The point becomes then one of finding $W_{class}(f)$ in the actual non-linear hysteretic material, an arduous objective, given that the solution of the diffusion equation coupled with a local dynamic hysteresis model, the method applied in non-oriented steel sheets [16,17], is hardly applicable to the coarse dw array of the HGO materials. Whatever the case, the statistical treatment discussed in [12] inevitably leads to the decomposition $W_{dyn}(f) = W_{class}(f) + W_{exc}(f)$ in the GO sheets, including the case of orientations different from the rolling direction [18,19]. In this work we shall simplify the matter by introducing the DC normal magnetization curve, taken as the magnetic constitutive equation of the material, in the electromagnetic diffusion equation and we shall calculate $W_{class}(f)$ accordingly. We shall associate the evolution of the dynamic losses versus f and J_p with stroboscopic Kerr observations of the surface domain structure. The Kerr experiments will provide a stringent test for the modeling of the dw dynamics, which will be carried out starting from the concept of dw bowing and its numerical implementation, for an array of equally spaced dws, bearing on Bishop's analysis of flexible, eddy current limited motion of single 180° dws [20,21].

Various phenomenological-empirical formulations have been proposed in recent and less recent times for dealing with broadband losses in magnetic sheets, many of them relying on variously modified Steinmetz's equation and the ensuing search for a more-or-less relevant number of fitting parameters or on extended experimental

characterization [22–25]. In the present work, where we investigate 0.174 mm and 0.289 mm thick sheets up to 10 kHz, we privilege the physical approach and the idea of loss decomposition, a concept preserving its meaning even in the presence of deep skin effect. The simulation of the behavior of the array of flexible dws upon increasing J_p and f permits one to predict the progressive transformation of the back-and-forth motion of the 180° dws (mode 1) into a moving horizontal front, separating a saturated band beneath the sheet surface from a nearly demagnetized inner core (mode 2), as sketched in Fig. 1. This justifies the correspondingly observed relative drop of $W_{exc}(f)$ in the upper (J_p, f) corner (e.g., 1.5 T at 5 kHz). A key role in such phenomena is evidently played by the sheet thickness.

2. Energy losses in HGO sheets up to 10 kHz and their interpretation

Hysteresis loops and losses were measured, under controlled sinusoidal polarization, between 1 Hz and 10 kHz on 0.174 mm and 0.289 mm thick HGO sheets. The polarization range 250 mT-1.7 T could be covered by combining Epstein frame and single strip testing. The 200 turns Epstein frame (IEC standard 60404–10) has been used up to 1 kHz, and a single Epstein strip tester with using local field measurements (H-coil) has been preferred at higher frequencies, because such a system allows for a significant decrease of the required apparent power [26]. Individual strips were then prepared for dynamic magneto-optical analysis, which was performed by means of a stroboscopic setup on the strip subjected to a defined exciting regime, the flux closure being ensured by a C-shaped laminated yoke. The domain structure was observed at selected points of the hysteresis loop on a 5 mm spot located on a well-oriented grain. Each image is obtained by averaging the individual frames and subtracting the background upon a few thousand successive cycles. The main features and the operating procedures of the employed fluxmetric and magneto-optical setups are fully discussed in [27].

The standard analysis by the STL of the energy loss versus frequency behavior in HGO sheets permits one to recognize incipient skin effect by the failure of Eq. (1) in data fitting. This generally occurs, depending on the sheet thickness, beyond power frequencies. One can then observe by Kerr imaging that the surface J_{psurf} and the bulk J_p peak polarization values increasingly diverge under increasing f, till the point where, depending on J_p, the material saturates at the surface for a fraction of the semi-period. This effect is apparent in Fig. 2, where the evolution along a semi-cycle of the surface domain structure in the 0.289 mm and 0.174 mm thick sheets is shown for $f = 5$ kHz and $J_p = 0.50$ T. The skin effect is manifest in the faster motion of the dws at the surface with respect to the bulk (dw bowing) and the partial disappearance of the surface domains at the tip points of this low-J_p cycle. By image analysis we get $J_{psurf} \sim$ 1.85 T and $J_{psurf} \sim 1.3$ T in the thicker and thinner sheet, respectively. J_{psurf} will obviously saturate under increasing J_p. The problem is therefore posed regarding the overall dw evolution versus J_p and f and
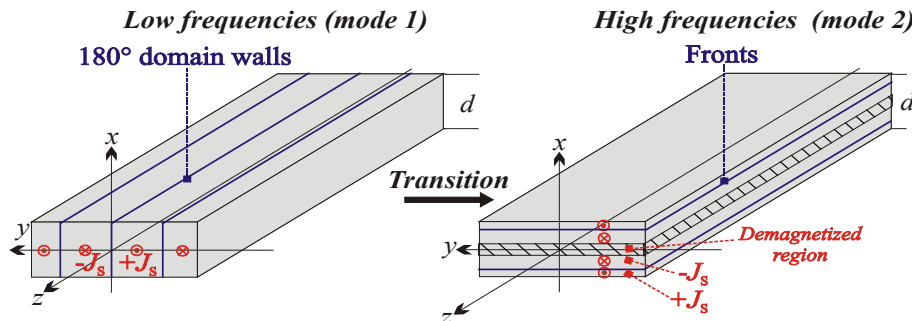

Fig. 1. The back-and-forth motion of the 180° dws occurring at power frequencies in HGO sheets (mode 1) evolves under increasing frequency via dw bowing and eventual merging at the sheet surface into a magnetization reversal carried out by a front propagating from surface to sheet midplane (mode2).
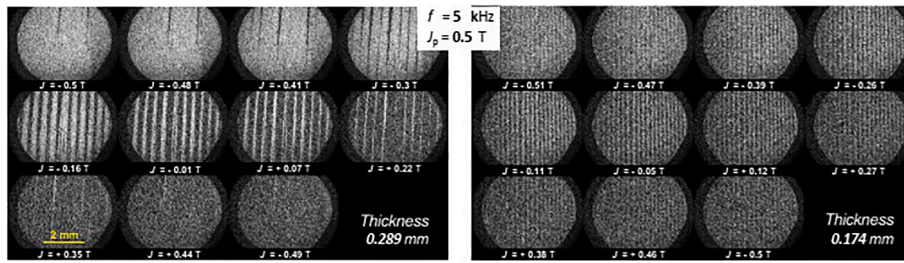
Fig. 2. Kerr imaging of the surface domain structure along a semi-cycle taken at 5 kHz and bulk peak polarization $J_p = 0.50$ T in the 0.289 mm and 0.174 mm thick HGO sheets. The surface peak polarization is estimated to attain the values 1.85 T and 1.3 T in the thicker and thinner strips, respectively. This quantity can fluctuate from grain to grain.

its modeling, which must be consistent with the Kerr observations and the macroscopic behavior of the GO sheets.

3. From domain wall bowing to the front-like mechanism

We assume a [0 0 1](1 1 0) infinitely extended single crystal endowed with regular anti-parallel 180° dws. At low frequencies the walls move back-and-forth under an alternating field, and can be assimilated, from the viewpoint of their dynamic behavior, as rigid objects (Pry&Bean model [28]). The Kerr results provide direct evidence of strong dw bowing and dw merging at the surface for sufficiently high ($J_p f$) product. Such conditions are largely met in the present experiments, thereby calling for an appropriate model for the dw motion, which we developed, starting from the classical Bishop's model [20,21], according to the following assumptions:

- The wall energy is $\gamma_w = 1.3 \bullet 10^{-3}$ J/m^2, and the electrical resistivity is $\rho = 48 \bullet 10^{-8}$ Ω·m. An infinite array of dws is considered, with spacing defined at each frequency by the Kerr observations.

- Each dw at rest is subdivided into $n = 128$ identical vertical elementary segments. The bowing of the dw under a changing applied field is then emulated, following Bishop's model, by connecting the vertical segments moving at different speed with horizontal segments, which allow for bowing by increasing their length on approaching the surface from the midplane. A dynamic balance is reached at any instant of time between the pressure exerted by the applied field and the counteracting effect by the eddy current field and the surface tension of the deformed wall. The eddy current field acting an any element is calculated by taking into account the contribution of the whole infinite array of equally moving 180° dws. The restoring force associated with the static coercivity does not play any role in this context. The mean dynamic dw spacing $2L$ is observed to decrease with the sheet thickness. We find, for example $2L \sim 0.24$ mm and $2L \sim 0.14$ mm in the 0.289 mm and 0.174 mm thick HGO sheets, respectively, at 5 kHz.

- At sufficiently high values of the product ($J_p \cdot f$) the bowing is severe and the dws collide at the sheet surface, where the magnetization tends to saturate (see Fig. 2). Further flux variation is therefore
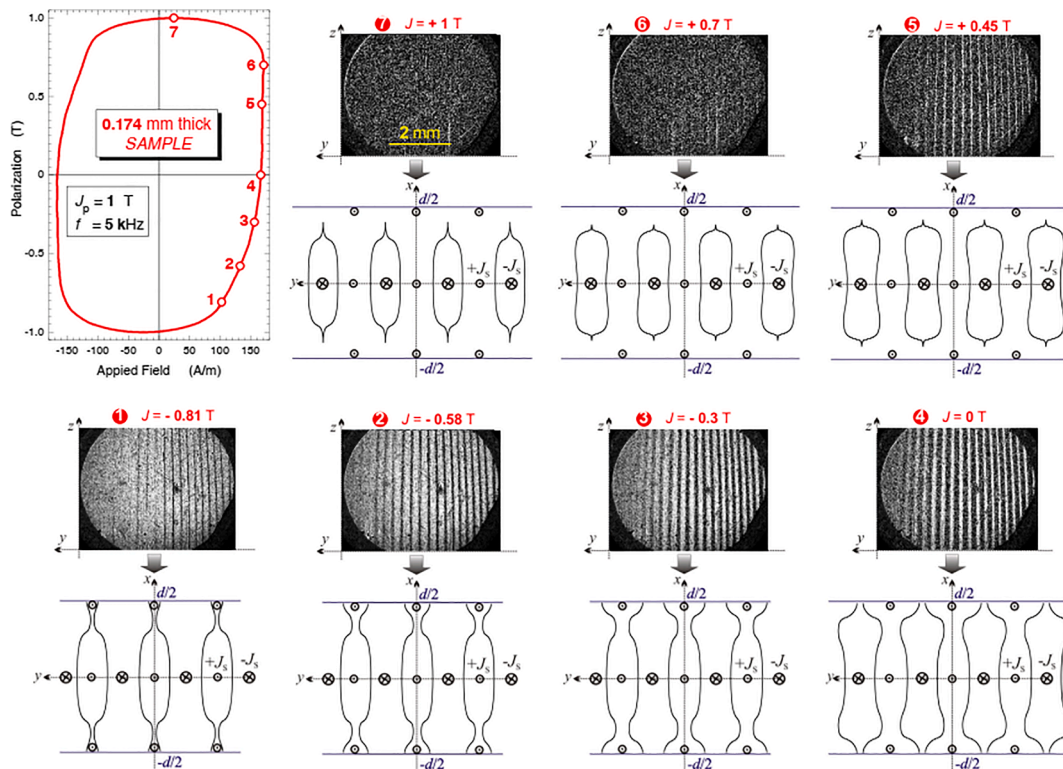

Fig. 3. 0.174 mm thick HGO sheet cyclically magnetized between ± 1.0 T at 5 kHz. The Kerr observation of the surface domain structure at different points of the ascending branch of the loop (*y-z* plane) is associated with a cross-sectional view (*x*-axis) of the corresponding evolution of the domain structure, as predicted by the numerical model of dw bowing.

ensured by the wall portions surviving in the bulk, which connect to form shrinking domains. It is the natural evolution of the bowing mechanism, which has been implemented in the code.

Fig. 3 provides a sequence of Kerr images of the surface domain structure, taken on the 0.174 mm thick sheet for $J_p = 1.0$ T and $f = 5$ kHz, at different points of the hysteresis loop. It is noted that the surface magnetization saturates for $J = J_p$. Each image is accompanied by the cross-sectional view of the correspondingly predicted profile of the domain structure ($-d/2 \leq x \leq d/2$), whose evolution along the ascending branch of the loop compares with the measured bulk magnetization and the Kerr results. Fluxmetric results, Kerr imaging, and theoretical prediction are shown to consistently fit in the example of Fig. 4, which deals with the characterization of the 0.289 mm thick sheet at 1.5 kHz for $J_p = 1.5$ T. To note the comparison between the Kerr images of the surface domains and the corresponding cross-sectional view of the theoretical domain structure at the points A and B of the ascending branch of the experimental loop (open symbols). The scenario is one pertaining to the upper (J_p, f) corner, where mode 2 is expected to prevail. The model shows that reverse domains are nucleated at the sheet surface upon returning from J_p (point A). They expand further under increasing reverse field, to eventually merge and cover the whole surface (point B), thereby forming a downward moving boundary (a horizontal undulating $180°$ dw), in analogy with the scheme sketched in Fig. 1. By plotting the rated sinusoidal $J(t)$ against the sustaining applied field $H_a(t)$ entering the dynamic dw model, we obtain substantial agreement with the experimental loop (red line in Fig. 4). To note that the quasi-static hysteresis provides negligible loss contribution at this frequency, while the the corresponding loop at $J_p = 1.5$ T is nearly square. It appears therefore appropriate to recognize the extent to which a classical calculation assuming a step-like $J(H)$ constitutive equation, entailing a perfect mode 2 magnetization process, can estimate the actual dynamic hysteresis loop. It is a simplest approach, for which there is analytical solution [12], leading to the inner loop (blue line) in Fig. 4 and therefore providing an acceptable prediction, but for the region immediately following the reversal (point A), where a small extra-area appears. This is what we expect, because the Kerr effect and the bowing model show a certain dw activity there. We can conclude that most of the energy loss is lumped into the classical term W_{cl} (although not predictable by Eq. (1)), but the small contribution by W_{exc} cannot be ignored.

Similar results can be found in the thinner GO sheet, although at

higher f and J_p values. The comparison of high frequency loops and losses given in Fig. 5 shows the great advantage of thinner sheets in terms of reduced losses. We shall prove in the following that this is mostly due to the strong decrease of $W_{class}(f)$.

4. Loss separation

We have previously stressed that the concept of classical loss $W_{class}(f)$ is physically justified in HGO sheets, despite their coarse domain structure. The difficult point remains, however, that of dealing with the actual non-linear hysteretic magnetic behavior of the material if $W_{class}(f)$ is to be calculated in the presence of skin effect. Some simplification should be attempted, by which one could connect, for example, the simple Eq. (1) at low frequencies with the step-like model at the highest polarization and frequency values. A possibility to cope with these two requirements is to define $W_{class}(f)$ as the quantity obtained by numerically solving the Maxwell's diffusion using the normal magnetization curve as the constitutive law of the material and determining a polarization profile $J(x)$ across the sample thickness [27]. The hysteresis loss component is then calculated by integrating $W_{hyst}(J(x))$, a quantity known from pre-emptive knowledge of the quasi-static loss upon an appropriately wide polarization range. Because of the non-uniform profile of $J(x)$, $W_{hyst}(J_p)$ is predicted to increase with f in the presence of skin effect. This could result into a somewhat overestimated $W_{hyst}(J_p)$ in the upper (J_p, f) corner, where the dw processes play a minor role (see Fig. 4). However, it is apparent in Fig. 6 that the contribution of $W_{hyst}(J_p)$ to $W(f)$ becomes in any case irrelevant. The excess loss $W_{exc}(f)$ is eventually obtained, for any J_p value, as the difference $W_{exc}(f) = W(f) - W_{hyst}(f) - W_{class}(f)$. The so-obtained loss decomposition, shown up to 10 kHz for $J_p = 1.7$ T in Fig. 6, shows that the large decrease of $W(f)$ observed in the thinner sheet at high frequencies (Fig. 5) chiefly comes
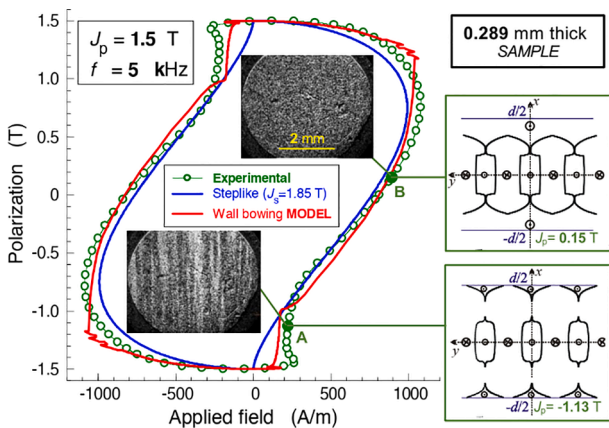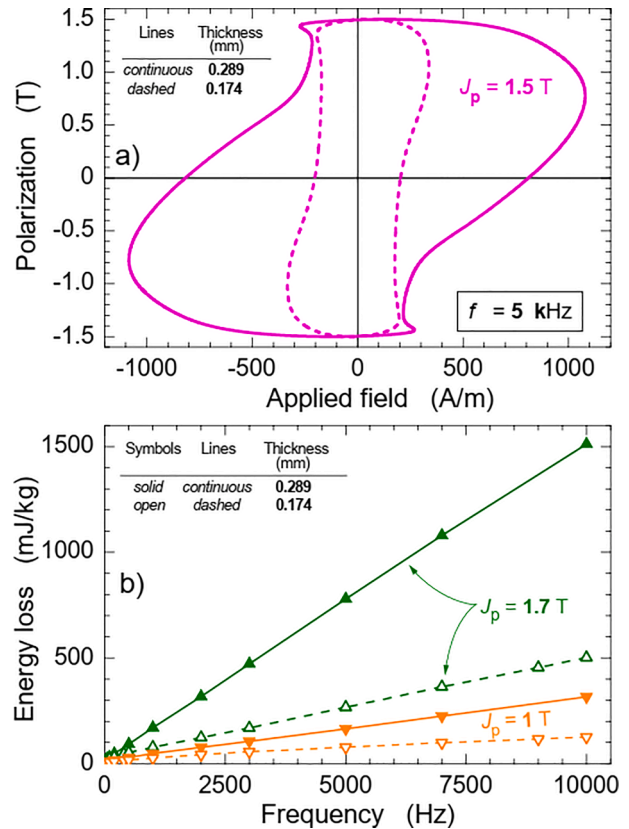

Fig. 4. 0.289 mm thick HGO sheet. The experimental cycle taken at $f = 5$ kHz for $J_p = 1.5$ T (open symbols) is compared with the loop calculated by the bowing model, accounting for wall periodicity and merging (red line), and the loop calculated according to the ideal case of step-like constitutive equation [12] (blue line). The surface domain structure by Kerr imaging associated with points A and B is compared with the cross-sectional view of the predicted domain structure. (For interpretation of the references to colour in this figure legend, the reader is referred to the web version of this article.)

Fig. 5. (a) Hysteresis loops measured at 5 kHz in the 0.289 mm and in the 0.17 mm thick samples for $J_p = 1.5$ T. (b) Energy loss $W(f)$ measured up to 10 kHz in the same sheet samples for $J_p = 1.0$ T and $J_p = 1.7$ T.
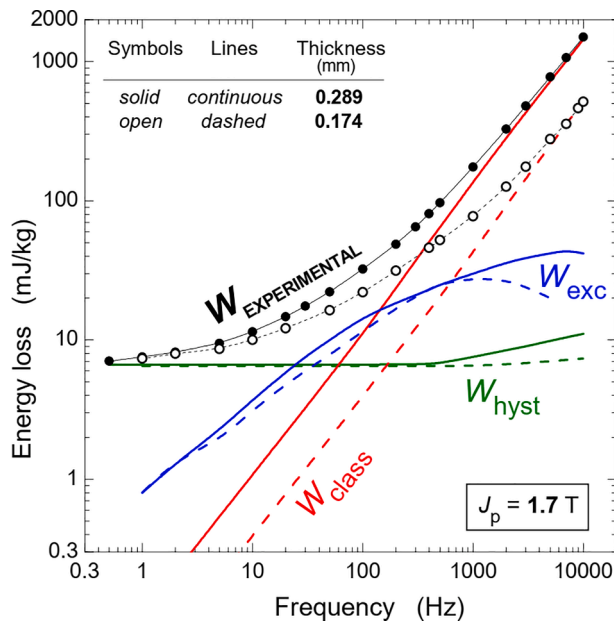
Fig. 6. Loss separation performed at 1.7 T up to 10 kHz in the 0.289 mm and 0.174 mm thick HGO sheets. The decrease of the measured $W(f)$ observed at high frequencies in the thinner sheets (see also Fig. 5b) is largely due to the corresponding decrease of $W_{class}(f)$, here calculated by taking the normal DC magnetization curve as the magnetic constitutive equation of the material. The hysteresis component W_{hyst} is predicted to increase at high frequencies, but it becomes, at the same time, inessential. $W_{exc}(f)$ shows instead a markedly restrained increase beyond a few hundred Hz, following the transition of the magnetization process from mode 1 to mode 2.

from a corresponding decrease of $W_{class}(f)$. It is associated with the transition of the magnetization process from mode 1 to mode 2, where the role of the dws, mainly connected with the domain nucleation at the point of reversal, becomes residual. $W_{exc}(f)$ correspondingly deviates from the low-frequency power law $W_{exc}(f) \propto f^n$, with $n \sim 0.6$, and flattens out, an effect occurring sooner in the thicker sheet.

From mode 1 to mode 2: some details.

We have shown that the transformation of the magnetization process from mode 1 to mode 2 is completed in the upper (J_p, f) corner. At low J_p and f values, the walls do not merge, while at sufficiently high frequencies a J_p value exists, for which two neighboring walls come in contact at their tip points at the sheet surface. By further increasing J_p, the walls merge and the sheet saturates across a horizontal band, thereby forming a domain arrangement reminding of the ideal mode 2 structure (see Fig. 4). An inner array of pseudo-elliptical domains, shrinking under the expanding horizontal band, ensures the existence of a near demagnetized region across the sheet core. At any frequency, the calculated fraction $\Delta t/T$ of the time period where the surface remains in the saturated state is predicted to increase with J_p, as shown in Fig. 7 (dashed lines). For a defined $\Delta t/T$ value, J_p and f follow an inverse relationship, where the hyperbolic parameter $k(\Delta t/T) = J_p f$ is observed to be larger, by virtue of the reduced eddy currents, in the thinner sheets. A few experimental points are provided in Fig. 7, where the (J_p, f) pairs identify $W_{exc}(f)$ values lower than 10 % of the dynamic losses. With $(\Delta t/T)$ occupying more than 60 % of the period, $W_{exc}(f)$ tends to disappear.

5. Conclusions

HGO Fe-Si sheets have been characterized up to 10 kHz by means of fluxmetric measurements and direct observations of the dw dynamics by stroboscopic Kerr investigations. The role of sheet thickness has been investigated by comparing the loss versus frequency behavior of 0.289 mm and 0.174 mm thick samples. The decomposition of the measured
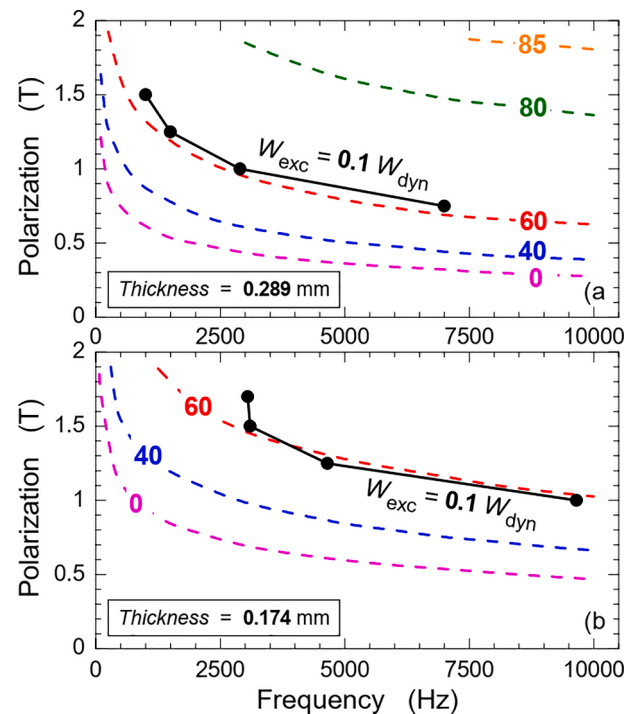

Fig. 7. The dashed lines show in percentage the calculated proportion of the magnetization period where the sheet surface is magnetically saturated (beneath the 0 line, no wall contact can occur). The solid line connects the (J_p, f) experimental points where the excess loss $W_{exc}(f)$ is reduced to 10 % of the dynamic loss. It is noted how the (J_p, f) corner moves upward in the thinner sheets.

loss $W(f)$ has been carried out for a range of peak polarization values J_p and evolving degree of flux penetration with frequency, which prevents the overall application of the standard formulation for the classical loss component $W_{class}(f)$. The Maxwell's diffusion equation has therefore been numerically solved by taking the normal magnetization curve as the magnetic constitutive equation of the material, thereby connecting in a continuous fashion low- and high-frequency response. A minor-to-marginal role by the dw-generated loss contributions (hysteresis and excess components) is thus predicted to occur, in all cases, beyond a few kHz. Consequently, the large decrease shown by $W(f)$ at high frequencies on passing from the 0.289 mm to the 0.174 mm thick sheets is chiefly associated with a corresponding decrease of $W_{class}(f)$. We consistently provide a microscopic interpretation of the loss phenomenology by focusing on the dw behavior, exploiting dynamic Kerr observations of the domains at the sheet surface, together with the modeling of the 180° wall motion. This is based on the notion of dw bowing and it permits one to provide a dynamic picture of the array of dws, where, on attaining the high (J_p, f) corner, the low-frequency back-and forth 180° dw oscillations (mode 1) pass through the merging of neighboring walls at the sheet surface and the creation of subsurface symmetric saturated horizontal bands, whose boundaries move towards the demagnetized sheet core under changing applied field. This is in rough analogy with the ideal magnetization mode 2, the one envisaged for a step-like $J(H)$ constitutive equation.

Declaration of Competing Interest

The authors declare that they have no known competing financial interests or personal relationships that could have appeared to influence the work reported in this paper.

Data availability

The data pertaining this research are available at the authors' laboratory.

References

[1] S. Taguchi, T. Yamamoto, A. Sakakura, New grain-oriented silicon steel with high permeability "ORIENTCORE HI-B", IEEE Trans. Magn. 10 (1974) 123–127, https://doi.org/10.1109/TMAG.1974.1058316.

[2] Y. Ushigami, M. Mikozami, M. Fujikura, T. Kubota, H. Fujii, K. Murakami, "Recent development of low-loss grain-oriented silicon steel, J. Magn. Magn. Mater. 254–255 (2003) 307–314, https://doi.org/10.1016/S0304-8853(02)00933-2.

[3] Z. Xia, Y. Kang, Q. Wang, Developments in the production of grain-oriented electrical steel, J. Magn. Magn. Mater. 320 (2008) 3229–3233, https://doi.org/10.1016/j.jmmm.2008.07.003.

[4] S. Takajo, T. Ito, T. Omura, S. Okabe, Loss and noise analysis of transformer comprising grooved grain-oriented silicon steel, IEEE Trans. Magn. 53 (9) (2017) 1–6.

[5] Q. Huang, M.L. Crow, G.T. Heydt, J.P. Zheng, S.J. Dale, The future renewable electric energy delivery and management (FREEDM) system: the energy internet, Proc. IEEE 99 (2011) 133–148, https://doi.org/10.1109/JPROC.2010.2081330.

[6] C. Zhao, D. Dujic, A. Mester, J.K. Steinke, M. Weiss, S. Lewdeni-Schmid, T. Chaudhuri, P. Stefanutti, Power electronic traction transformer—medium voltage prototype, IEEE Trans. Ind. Electr. 61 (2014) 3257–3268, https://doi.org/10.1109/TIE.2013.2278960.

[7] M.A, Hannan, P.J, Ker, M.H, Lipu, Z.H, Choi, M.S.A, Rahman, K.M, Muttaqi, F, Blaabjerg, State of the art of solid state transformers: advanced topologies, implementations issues, recent progress and improvements, *IEEE Access*, 8 (2020) 19113 – 19132. https://doi.org/ 10.1109/ACCESS.2020.2967345.

[8] N. Soltau, D. Eggers, K. Hameyer, R.W. De Doncker, Iron losses in a medium-frequency transformer operated in a high-power DC–DC Converter, IEEE Trans. Magn. 50 (2) (2014) 953–956.

[9] T. Belgrand, R. Lemaître, A. Benabou, J. Blaszkowski, C. Wang, Thin grain oriented electrical steel for PWM voltages fed magnetic cores, AIP Advances 8 (4) (2018) 047611.

[10] H. Ichou, D. Roger, M. Rossi, T. Belgrand, R. Lemaitre, Assessment of a grain oriented wound core transformer for solid state converter, J. Magn. Magn. Mater. 504 (2020) 166658.

[11] G. Bertotti, General properties of power losses in soft ferromagnetic materials, IEEE Tran. Magn. 24 (1988) 621–630, https://doi.org/10.1109/20.43994.

[12] G. Bertotti, Hysteresis in Magnetism, CA, Academic Press, San Diego, 1998.

[13] S. Steentjes, S.E. Zirka, Y.E. Moroz, E.Y. Moroz, K. Hameyer, Dynamic magnetization model of nonoriented steel sheets, IEEE Tran. Magn. 50 (4) (2014) 1–4.

[14] S.E. Zirka, Y.I. Moroz, S. Steentjes, K. Hameyer, K. Chwastek, S. Zurek, R. G. Harrison, Dynamic magnetization model for soft ferromagnetic materials with coarse and fine domain structure, J. Magn. Magn. Mater 394 (2015) 229–236, https://doi.org/10.1016/j.jmmm.2015.06.082.

[15] C. Ragusa, H. Zhao, C. Appino, M. Khan, O. de la Barriere, F. Fiorillo, Loss decomposition in non-oriented steel sheets: the role of the classical losses, IEEE Magn. Lett. 7 (2016) 1–5.

[16] V. Basso, G. Bertotti, O. Bottauscio, M. Chiampi, F. Fiorillo, M. Pasquale, M. Repetto, Power losses in magnetic laminations with hysteresis: finite element modelling and experimental validation, J. Appl. Phys. 81 (1997) 5606–5608, https://doi.org/10.1063/1.364614.

[17] L.R. Dupre, O. Bottauscio, M. Chiampi, M. Repetto, J.A.A. Melkebeek, Modeling of electromagnetic phenomena in soft magnetic materials under unidirectional time periodic flux excitations, IEEE Trans. Magn. 35 (5) (1999) 4171–4184.

[18] C. Appino, E. Ferrara, F. Fiorillo, C. Ragusa, O. de la Barrière, Static and dynamic energy losses along different directions in GO steel sheets, J. Magn. Magn. Mater. 500 (2020), 166281, https://doi.org/10.1016/j.jmmm.2019.166281.

[19] E. Ferrara, C. Appino, C. Ragusa, O. de la Barrière, F. Fiorillo, Anisotropy of losses in grain-oriented Fe-Si, AIP Adv. 11 (11) (2021) 115208.

[20] J.E.L. Bishop, Understanding magnetization losses in terms of eddy current dominated domain wall dynamics, J. Magn. Magn. Mater. 19 (1980) 336–344, https://doi.org/10.1016/0304-8853(80)90626-5.

[21] J.E.L. Bishop, Modelling domain wall motion in soft magnetic alloys, J. Magn. Magn. Mater. 41 (1984) 261–271, https://doi.org/10.1016/0304-8853(84)90193-8.

[22] O, Messal, A, Kedous-Lebouc, O, Geoffroy, P, Mas, H, Dhahbi, C, Chillet, S, Buffat, S, RandI, Analysis of the Dynamic Behavior of Magnetic Materials Under High B and dB/dt. *Soft Magnetic Materials Conference SMM23*, Sept. 2017, Séville, Spain (hal-01589353).

[23] J, Mülethaler, J, Biela, J.W, Kolar, J.W, Ecklebe, A. Improved core loss calculation for magnetic components employed in power electronic systems. *IEEE Trans. Power. Electron.* **2012**, *27*, 964–973. https://doi.org/10.1109/TPEL.2011.2162252.

[24] W. Guan, H. Kong, M. Jin, L. Lan, Z. Du, Y. Zhang, J. Ruan, H. Zhang, Anal.ysis of excess loss in SiFe laminations considering eddy-current dominated domain wall motion, IEEE Trans. Magn. 51 (3) (2015) 1–4.

[25] B. Ducharne, P. Tsafack, Y.A. Tene Deffo, B. Zhang, G. Sebald, Fractional operators for the magnetic dynamic behavior of ferromagnetic specimens: an overview, AIP Adv. 11 (2021), 035309, https://doi.org/10.1063/90000044.

[26] O. de la Barrière, C. Ragusa, M. Khan, C. Appino, F. Fiorillo, F. Mazaleyrat, A simple compensation method for the accurate measurement of magnetic losses with a single strip tester, IEEE Trans. Magnetics 52 (5) (2016) 1–4.

[27] A. Magni, A. Sola, O. de la Barrière, E. Ferrara, L. Martino, C. Ragusa, C. Appino, F. Fiorillo, Domain structure and energy losses up to 10 kHz in grain-oriented Fe-Si sheets", AIP Adv. 11 (2021), 015220 https://doi.org/10.1063/9.0000184.

[28] R.H. Pry, C.P. Bean, Calculation of the energy loss in magnetic sheet materials using a domain model, J. Appl. Phys. 29 (1958) 532–533, https://doi.org/10.1063/1.1723212.